Thermal Evaporated Undoped and Na-doped $CuInS_2$ with Copper Contact for Photovoltaic Applications

Jackson LONTCHI‡, Bilel KHALFALLAH, Mohamed ABAAB

Université Tunis El Manar, Ecole Nationale d'Ingénieurs de Tunis, Laboratoire de Photovoltaïque et matériaux semiconducteur, 1002, Tunis, Tunisie

(jacksonlontchi@yahoo.fr, bilel_khalfallah@yahoo.com, mohamed.abaab@enit.rnu.tn)

‡ Corresponding Author; Jackson LONTCHI, BP 37, belvedere 1002-ENIT Tunis, Tunisia, Tel: +216 94772882, jacksonlontchi@yahoo.fr

Received: 24.02.2016 Accepted: 07.05.2016

Abstract- Undoped and Na-doped $CuInS_2$ powder has been synthetized by direct fusion of precursor elements. We have deposited those two materials in thin films on glass substrate and on copper layer by vaccum thermal evaporation method followed by an annealing in air atmosphere at 250°C and 450°C. We have investigated their structural, optical and electrical properties that show good results for photovoltaic applications. The undoped $CuInS_2$ layer exhibit an n-type conductivity whereas Na-doped $CuInS_2$ is p-type both on glass and on copper layer. X-ray analyses of the as deposited samples show amorphous structures. The annealed samples in air showed a crystalized $CuInS_2$ layer with a major peak of the (112) chalcopyrite phase with the presence of CuO and In_2S_3 impurity phases for the 450° annealed. Optical gap of both undoped and Na-doped $CuInS_2$ where between 1.4 and 1.6 eV, that is close to the optimal gap value 1.5 eV of the $CuInS_2$ suitable for a good absorption of solar spectrum. Electrical characterizations showed good ohmic contacts with low potential barrier height, and good ideality factor of respectively (0.75 eV, 1.37) for undoped and (0.66 eV, 1.27) for Na-doped $CuInS_2$/Cu contacts. Also, we observed a low value of series resistance 3.51 and 1.75 Ohms respectively that suppose a good current flow in the contact.

Keywords- Metal semi-conductor, $CuInS_2$/Cu, Na doping, structural, optical, electrical.

1. Introduction

Research in thin film solar cells is growing and new materials are been studying, but many researchers are still working on $CuInS_2$ solar cells because it's still a promising material for solar cell with its optimal direct band gap of 1.5 eV that match's well with the solar spectrum [1] and it's high absorption coefficient of around 10^{-5} cm^{-1} [2]. Metal-semiconductors back contact plays an important role in the efficiency of the solar cell; it's responsible of the flow and the collect of the generated electron-hole pairs responsible of the current produced by the cell. Many metals have been studied as back contacts with $CuInS_2$ in the literature such as Aluminium (Al), Carbone (C), Gold (Au), Silver (Ag), Molybdenum (Mo), Indium (In), Copper (Cu) [3-5]. Contacts on $CuInS_2$ made with aluminum were found to be Schottky as shown by *J. M. Peza-Tapia et al.* [4]. They reported in the same article good ohmic contacts with Ag and In metals with a low value of specific contact resistivity for the In contact with $CuInS_2$. *D. C. Nguyen et al.* [3] reported different efficiency for solar cell based on $CuInS_2$ with different metals back contacts (Al, Cu, Mo and Au deposited by rf sputtering and Carbon back contact by screen printing). Al and Au had the lower efficiency of 1.96 and 1.87 % respectively, back contact with Cu and Mo gave better efficiency (2.17 and 2.08 %) that make them good candidates for back contact in CIS solar cells.

Molybdenum back contact is the most used and has given good efficiency in CIS solar cells until today. Best efficiency of 12.5 % has been achieved on Mo/$CuInS_2$/CdS/ZnO cell [6] but that type of cells contains toxic and cost elements. An important research goal in photovoltaic devices is the replacement of costly and toxic materials by nontoxic and cheap materials [7] to make clean, efficient and cheap solar cells available for most of the world population.

Copper is a low cost and non-toxic metal that has good electrical properties suitable for current conduction. He has an easy oxidation in air atmosphere, but used as back contact this property can be hidden by the top layer. That why many researchers have tried to use it as back contact in thin film solar cells based on $CuInS_2$.

The first report of copper as back contact with $CuInS_2$ was in 1998 and 2001 by *J. Penndorf, M. Winkler et al.* [8, 9], they first reached an efficiency of around 6%. Since then, many studies have been made to improve the quality of the $CuInS_2$/Cu back contact [10-15] by roll-to-roll process that was found to be a low-cost method able to produce large scale and event flexible cells but has the disadvantage of instability.

Vacuum thermal evaporation deposition has been found to be a good method to produce good quality and stable semi-conductor thin films. *M. B. Rabeh et al.* [16] have obtained good quality $CuInS_2$ thin films by vacuum thermal evaporation followed by annealing in air atmosphere.

We report here, the structural, optical and electrical characterization of undoped and Na-doped $CuInS_2$ thin films and metal-semiconductor contact with Copper deposited by vacuum thermal evaporation followed by an annealing in air atmosphere at 250°C and 450°C. Na doping is performed in order to introduce acceptors atoms to convert the type of conductivity from n to p-type.

2. Experience

2.1. Synthesis of $CuInS_2$ powder

Undoped and Na-doped $CuInS_2$ powder was synthetized by direct fusion of precursor elements. For the Undoped, precursor elements Cu, In and S of 99,999% purity were sealed in a vacuum quartz tube in atomic stoichiometric proportions. The melt was heated in a programmable furnace first slowly at 20°C/h rate in order to avoid explosion due to sulphur vapor pressure, after a stabilization of the melt at 600°C for 24h, the complete homogenization was obtained after keeping at 1000°C for 48h then followed by a cooling at 10°C/h till 800°C before the natural cooling till ambient temperature. For the Na-doped, we added pure sodium element into the quartz ampoule containing the stoichiometric precursor's elements Cu, In, S at 1 atomic percent (1 at. %) according to the good results obtained by *M. Zribi et al.* [17]. Crushed powder of both undoped and Na-doped $CuInS_2$ was used as raw materials for the thermal evaporation.

2.2. Contacts preparation

Thin film layers were grown by vacuum thermal evaporation on unheated glass substrates using a highly resistive tungsten crucible in a high vacuum evaporation system at a pressure of ~10^{-5} Torr. We have deposited undoped and Na-doped $CuInS_2$ powder on unheated glass substrates in order to characterize the $CuInS_2$ layer. In order to form the metal semiconductor contact, around 100 mg of small copper pelts of 99,999% purity was evaporated on glass to form the copper layer. $CuInS_2$ was then evaporated on top of the copper layer in order to form the contact. The $CuInS_2$ layer was deposited on 80% of the copper surface in order to leave a free surface for the Cu-electrodes during electrical characterizations. To improve the crystallinity of the films and make sure we are dealing with good quality of $CuInS_2$, the samples were annealed in air atmosphere at 250°C and 450°C for 2h in a programmable furnace of Nabertherm type.

2.3. Contact characterizations

We have investigated the structural properties of the undoped and Na-doped $CuInS_2$ films on glass substrate and with copper contact by X-ray diffraction (XRD) using a D8 advance diffractometer with CuK_α radiation. Optical transmittance and reflectance of the $CuInS_2$ layers on glass substrates were determined with a UV-VIS-NIR spectrophotometer of type Shimadzu 3100S in the range of 300-1800 nm. The type of conductivity of the $CuInS_2$ layer on glass substrates and copper was determined by the hot probe method. Current-voltage characterization of metal-semiconductor contacts was performed with an Agilent N6762A source-measure unit at ambient temperature.

3. Results And Discussion

3.1. Structural properties

Fig. 1 shows the XRD patterns of undoped $CuInS_2$ thin films as deposited, annealed at 250°C and 450°C in air atmosphere. We observe that the as deposited layer has an amorphous structure without any diffraction peak. This amorphous structure of $CuInS_2$ as deposited on unheated glass substrates has already been reported in previous work [18, 19]. After annealing at 250°C for 2h in air, we observe a growth of three peaks attributed to the $CuInS_2$ where the major peaks is the (112) at $2\theta = 27.93°$ that indicate the majorly chalcopyrite phase of the film with a secondary InS (541) phase which disappear at 450°C. Two copper oxide CuO (-111) and (200) phases are observed at 450°C that can be explained by the reaction at high temperature between copper atoms and oxygen atoms present in the air atmosphere. The In_2S_3 may be related to the lack of copper that has been oxided that left a Cu poor phase in the film. We noted a decrease in the intensity of the preferential (112) peak at 450°C that reflect a decrease of the crystallinity may be due to the presence of CuO and InS secondary phases in the material.

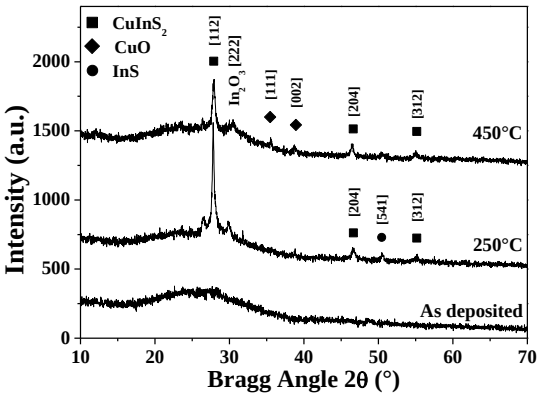

Fig. 1. XRD patterns of undoped $CuInS_2$ deposited on glass substrates.

Fig. 2 shows the XRD patterns of the Na-doped $CuInS_2$ on glass substrates as deposited and annealed at 250°C and 450°C in air atmosphere. The as deposited sample exhibit an amorphous structure like the undoped but the 250°C annealed one is also amorphous may be due to the presence of Na atoms in the structure who have difficulties to integrate the sites of the matrix may be due to the great value of the radius of Na atom (190pm) related to Cu atomic radius (128pm). The 450°C annealed sample shows a mixture of two chalcopyrite phases $CuInS_2$ and $CuIn_5S_8$ with the preferential peak for the $CuInS_2$ (112). The presence of the $CuIn_5S_8$ as a minor phase in Na doped $CuInS_2$ has already been reported in the literature as impurity phase [20, 21]. Another explanation could be that Na atoms integrate the matrix and occupied Cu lattices sites and leave Cu vacancies that lead to $CuIn_5S_8$ phase.

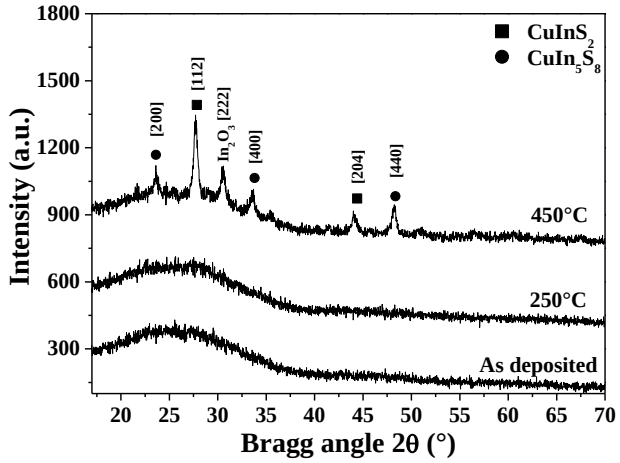

Fig. 2. XRD patterns of Na-doped $CuInS_2$ deposited on glass substrates.

The size of the crystallites in the grains were estimated by the Debye-Scherrer formula [22] :

$$D = \frac{0.9\lambda}{\beta \cos\theta} \quad (1)$$

Where λ is the X-ray wavelength of 1.5418 Å, θ is the Bragg diffraction angle and β is the Full Width at Half Maximum (FWHM).

The values of the crystallites sizes and their correspondent FWHM are listed in table 1 were we observed a decrease of the crystallite sizes with the annealing temperature.

Table 1. Bragg angles, FHWM, grains sizes, for undoped and Na-doped $CuInS_2$ as deposited and annealed at 250°C and 450°C.

$CuInS_2$ samples	Annealed T(°C)	Bragg Angles (°C)	FHWM	Grains sizes (nm)
Un doped	As dep.	-	-	-
	250°C	27.82	0.117	122.02
	450°C	27.93	0.267	53.43
Na doped	As dep.	-	-	-
	250°C	-	-	-
	450°C	27.70	0.334	42.71

Fig. 3 shows XRD patterns of undoped $CuInS_2$ deposited on copper layer. An amorphous $CuInS_2$ phase is observed on the as deposited samples as already seen in XRD patterns of $CuInS_2$ on glass substrate. But, there are two peaks in the patterns that has been identified as Cu (111) and Cu (200) at $2\theta = 43.39$ and 50.58° respectively. This confirms the presence of a copper layer in the structure. After annealed at 250°C, we observed the growth of $CuInS_2$ peaks with the (112) one that is preferential. But still the copper peaks are observed due to the semi crystallized $CuInS_2$ layer. In the 450°C annealed sample, there are no copper peaks indicating a good crystallization of the $CuInS_2$ layer with its preferential chalcopyrite (112) peak that hides the copper layer from the X-rays. We noted here the preferential (112) peak of $CuInS_2$ of the 450°C annealed sample is more intense than the 250° annealed one, contrary to the case of the $CuInS_2$ layer deposited on glass substrate where the (112) peaks was less intense at 450°C. This may be due to the diffusion of copper atoms from the copper under layer in the $CuInS_2$ layer that compensate the lack of Cu and ameliorates the crystallinity of the $CuInS_2$ layer. We noticed here the benefit effect of the copper under layer which plays a copper atoms tank role for the $CuInS_2$. Copper oxide impurities due to the oxidation in air atmosphere that contribute to the decrease in crystallinity.

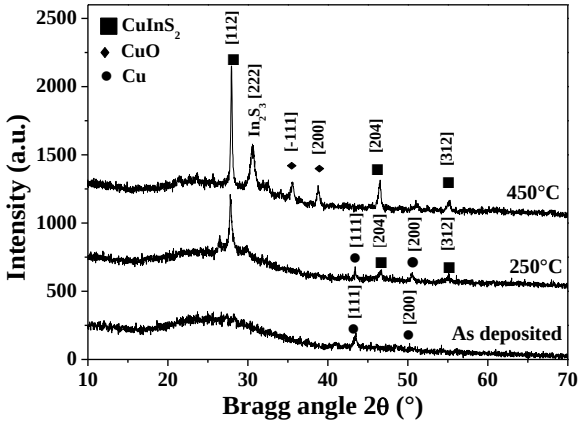

Fig. 3 . XRD patterns of undoped $CuInS_2$ on copper layer.

The same observation is done with the XRD patterns of Na-doped $CuInS_2$ on copper substrate on fig. 4 were the as deposited and the 250°C annealed sample shows an amorphous structure with the presence of Cu (111) peak. The Cu peaks disappear after annealed at 450°C and the $CuInS_2$ (112) peak is major. We also have the CuO (111)/(200) and the In_2S_3 (222) phases as for the Na-doped $CuInS_2$ on glass substrate. We noticed the absence of $CuIn_5S_8$ phases on the 450°C annealed sample comparatively to the sample on glass substrate may be due to the diffusion of Cu atoms coming from the Cu layer that has form a Cu-rich layer compensating the lack of Cu atoms in the $CuIn_5S_8$ phases. We note here again another benefit effect of the copper under layer on the $CuInS_2$ thin film.

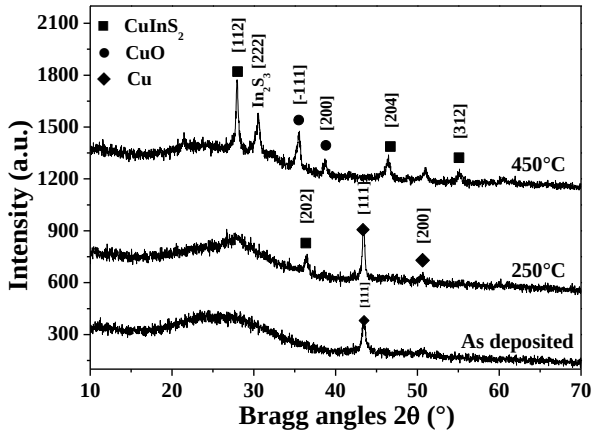

Fig. 4 . XRD patterns of Na-doped $CuInS_2$ on copper layer.

3.2. Optical properties

We have measured the optical transmittance and reflectance in the range of 300 nm to 1800 nm for the as deposited and annealed samples of undoped and Na-doped $CuInS_2$ on glass substrates (fig. 5, fig. 6). The reflectance for both undoped and Na-doped are in the range of 10 to 40%, while the transmittance rise till 80% and 88% for the as deposited and the 250°C annealed samples and just to 60% and 70% for the 450°C annealed undoped and Na-doped samples respectively. We noted a loss of oscillations for the 450°C annealed undoped sample that confirm the decrease of crystallinity observed in the XRD patterns due to the secondary oxide phases. All the Na-doped spectra shows oscillations even the 450°C annealed one sign of a good homogeneity of the film. The absorption coefficients of all the $CuInS_2$ samples were in the range of 10^5 cm^{-1} that is suitable for high solar spectrum absorption.

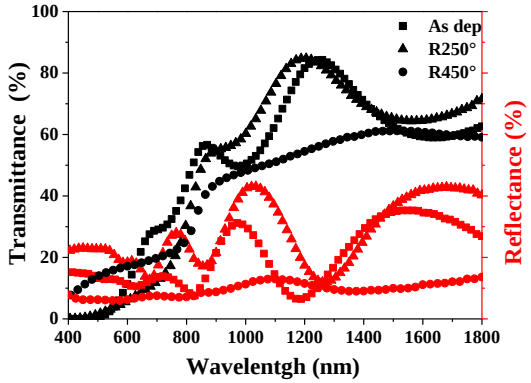

Fig. 5. Transmittance and reflectance of the undoped $CuInS_2$ on glass substrates.

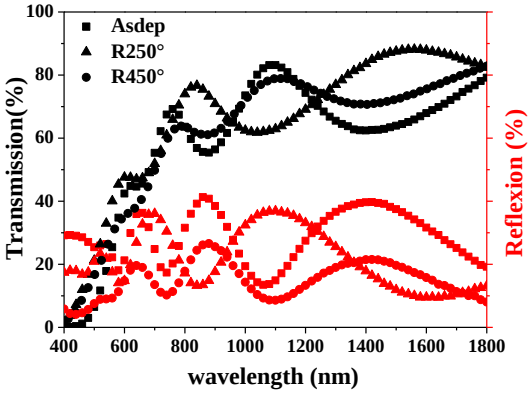

Fig. 6. Transmittance and reflectance of the Na-doped $CuInS_2$ on glass substrates.

The average film thickness and refractive index of the undoped and Na-doped films were calculated by the interference fringes method [23] the average values are listed in table 2.

Table 2. Film thickness and refractive index of undoped and Na-doped $CuInS_2$ on glass substrates.

$CuInS_2$ samples	Annealed T(°C)	Film thickness (nm)	Refractive index
Un doped	As dep.	287.19	2.51
	250	164.54	2.36
	450	159.76	1.70
Na doped	As dep.	249.63	2.65
	250	110.36	2.46
	450	104.78	1.87

The optical band gap was calculated by the Tauc model [24], and the Davis and Mott model [25] in high absorbance region given by the relation:

$$(\alpha h\nu)^n = A(h\nu - E_g) \quad (2)$$

Where A is a constant, $h\nu$ the photon energy, α is the absorption coefficient and E_g the optical band gap. n is a coefficient depending on the type of transition allowed in the film $n = 2$ for a direct transition allowed and $n = ½$ for an indirect transition allowed. The plot of $(\alpha h\nu)^2$ vs $h\nu$ yields a straight line that indicate in the abscise axis the average value of the band gap. Fig. 7 and fig. 8 show the plots of $(\alpha h\nu)^2$ vs $h\nu$ for all the undoped and Na-doped samples. We noted a decrease of band gap value with the annealing temperature due the improvement of the crystallinity of the films. Values are between 1.3 eV and 1.6 eV around the optimal band gap value of the $CuInS_2$ suitable for solar spectrum absorption for photovoltaic applications.

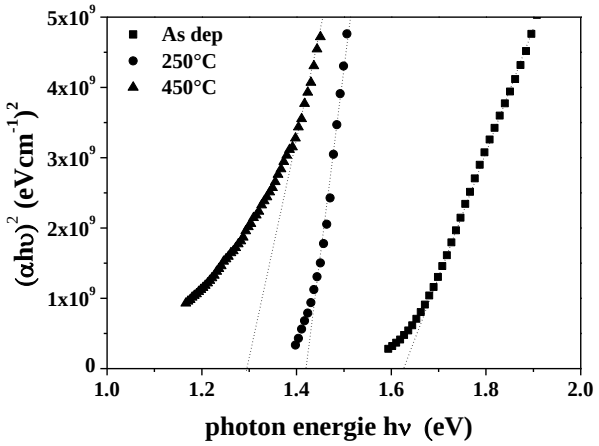

Fig. 7 . Optical band gap for undoped $CuInS_2$ as deposited, 250°C and 450°C annealed.

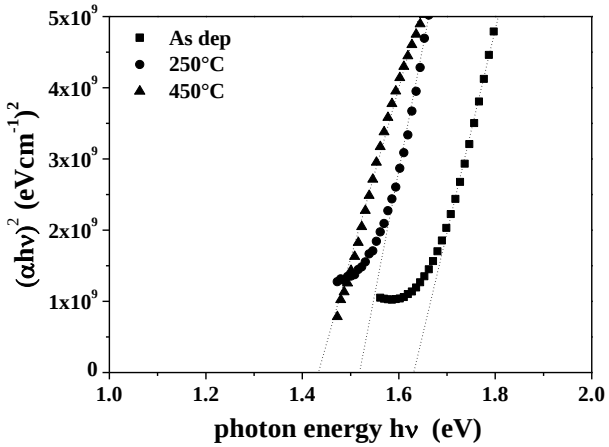

Fig. 8. Optical band gap for Na-doped $CuInS_2$ as deposited, 250°C and 450°C annealed.

The hot probe method was used to determine the type of conductivity of the major carrier for the undoped and Na-doped $CuInS_2$ on glass substrate. The undoped $CuInS_2$ layer was n type and the Na-doped was p type either on glass substrates than on copper layer. They can then be combining with p or n-type oxide transparent conductor in photovoltaic solar cell applications.

3.3. Electrical properties

We have measured the current-voltage (I-V) characteristic of the contact with our source measure unit at ambient temperature. The I-V curves are shown on fig. 9 and fig. 10 for the undoped and the Na-doped $CuInS_2$ contact with copper respectively. Both curves showed linear characteristic that means a good ohmic contacts suitable for photovoltaic back contacts.

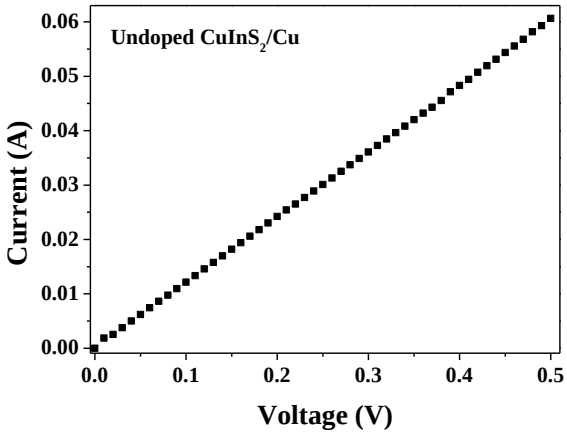

Fig. 9 . current-voltage characteristic of the undoped $CuInS_2$ contact with copper.

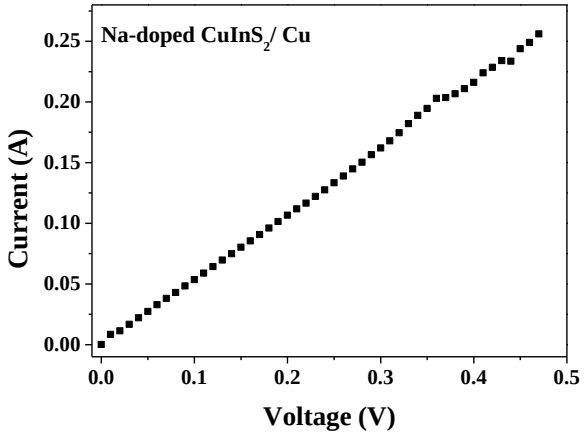

Fig. 10. Current-voltage characteristic of the Na-doped $CuInS_2$ contact with copper.

The saturation current has been determinate by our measurement unit as the current value when V = 0. The values are listed in TABLE 2. They are in the range of 10^{-6}, 10^{-5} (A) respectively for the undoped and the Na-doped $CuInS_2$ contact.

The potential barrier height, the ideality factor and the series resistance of the contact have been investigated by the Schottky model [26] assuming the thermionic emission

is the predominant mechanism of conduction in the contact that is usually for and ideality factor between 1 and 2 [27]. The relationship between the current I and the voltage V is given by the formula :

$$I = I_s\left(\exp(\frac{qV}{nkT}) - 1\right) \quad (3)$$

Where I_s is the saturation current, q the electron charge, n the ideality factor, k the Boltzmann constant and T the temperature.

The potential barrier height ϕ_b is given in the expression of the saturation current I_s :

$$I_s = AA^*T^2\exp\left(-\frac{q\phi_b}{kT}\right) \quad (4)$$

Where A is the area of the contact, A^* the Richardson constant of the semiconductor material.

The potential barrier values are respectively 0.75 and 0.66 eV for undoped and Na-doped $CuInS_2$ contacts. These barrier values are lows, that suppose the existence of a weak barrier of potential between the $CuInS_2$ layer and the copper that suppose a good flow of current in the contact.

The values of the ideality factor n where obtained from the slope of the linear region of the plot of Ln(I) vs V in the low voltage region. The ideality factor values are 1.37 and 1.27 respectively. They are between 1 and 2 that confirm the use of the Schottky thermionic emission theory and they are close to the ideal value 1 that supposes a good diode contact fabrication and few defects in the contact.

We have determinate the series resistance of the contacts that gives an indication of the opposition of the current flow in the contact due to the contact and the electrodes. The series resistance is expressed by the relation:

$$\frac{dV}{dLn(I)} = R_s I + \frac{nkT}{q} \quad (5)$$

R_s is the slope of the linear region of the curve of *V/Ln(I)* vs *I*. the values obtained are 3.51 and 1.75 **Ω**. This supposes a good flow of charges between the electrodes and the contact layers that is good for photovoltaic applications where we need to collect the maximum of the electrons-holes pairs generated in the cell to produce current.

Table 2. Saturation current, potential barrier height, ideality factor and series resistance of undoped and Na-doped $CuInS_2$ contact with copper.

Contact material	Is (A)	ϕ_b (eV)	n	R_s (Ω)
Undoped $CuInS_2$/Cu	$3.75\ 10^{-6}$	0.75	1.37	3.51
Na-doped $CuInS_2$/Cu	$7.02\ 10^{-5}$	0.66	1.27	1.75

4. Conclusion

We have synthetized undoped and 1% at. Na-doped $CuInS_2$ material by direct fusion of precursor elements and we have made metal semiconductor contacts with copper metal layer by thermal evaporation followed by an annealing in air atmosphere at 250°C and 450°C. We have characterized the undoped and the Na-doped $CuInS_2$ layer on glass substrate and the contact with copper. The results of the characterization of the $CuInS_2$ layer on glass substrates gave thin film with band gap value between 1.4 and 1.6 eV and absorption coefficient in the range of 10^5 cm^{-1} that are suitable as absorber layer for photovoltaic applications. Structural investigations of the undoped and Na-doped $CuInS_2$ layer on glass showed an amorphous structure for the as deposited samples but the 450°C annealed one were crystallized with the major peak attributed to the (112) $CuInS_2$ chalcopyrite phase. The structural properties of the contacts with copper shown the same patterns with the presence of the Cu (111) and (200) peaks for the as deposited and the 250°C annealed samples. The Cu peak disappears in the 450°C annealed pattern and the $CuInS_2$ (112) peak is still major. The electrical studies showed good result for the potential barrier height, the ideality factor and series resistance. The low value of the barrier supposes an easier passage of charges between Cu metal and $CuInS_2$ semiconductor. The ideality factor close to 1 let suppose a good contact fabrication with few defaults. The low value of series resistance let think of a good flow of charges between the electrodes and the layers of the contact. All those properties make the undoped and Na-doped $CuInS_2$ thin films good n and p-type absorber layers and metal back contact with copper could be good candidate for photovoltaic solar cell applications.

References

[1] W. Ligang, W. Yanlai, Y. Wei, Z. Jun, X. Jingang, Rare Metal Materials and Engineering, 44(4), pp. 0805-0807, 2015.

[2] C. O. Mosiori, Rift Vally Journal of science and technology, 1, 2, 2015.

[3] D.-C. Nguyen, K. Takehara, T. Ryo, S. Ito, Energy Procedia, 10, pp. 49 – 54, 2011.

[4] J. M. Peza-Tapia, A. Morales-Acevedo, M. Ortega-Lopez, Solar Energy Materials & Solar Cells, 93, pp. 544–548, 2009.

[5] A. Opanowicz, B. Koscielniak-Mucha, Phys. Stat. Sol. (a), 105, K135, 1988.

[6] J. Klaer, J. Bruns, R. Henninger, K. Seimer, R. Klenk, K. Ellmer, D. Braunig. Semicond. Sci. and Tech.13, 8, pp. 1456, 1998.

[7] A. S. Cherian, T. Abe, Y. Kashiwaba, C. S. Kartha, K. P. Vijayakumar, Energy Procedia 15, pp. 283–290, 2012.

[8] J. Penndorf, M. Winkler, O. Tober, D. Röser, K. Jacobs, Solar Energy Materials and Solar Cells, 53, pp. 285-298, 1998.

[9] M. Winkler, J. Griesche, O. Tober, J. Penndorf, E. Blechschmied, K. Szulzewsky, Thin Solid Films, 387, pp. 86-88, 2001.

[10] J. Wienke, V. Groen-Smita, M. Burgelman, S. Degrave, J. Penndorf, Thin Solid Films, 387, pp. 165-168, 2001.

[11] J. Verschraegen, M. Burgelman1, J. Penndorf, Thin Solid Films, 451– 452, pp. 179–183, 2004.
[12] M. Winkler, J. Griesche, I. Konovalov, J. Penndorf, J. Wienke, O. Tober, Solar Energy, 77, pp. 705-716, 2004.
[13] J. Verschraegen, M. Burgelman1, J. Penndorf, 20th European Photovoltaic Solar Energy Conference, Barcelona, Spain, 6 –10, June 2005.
[14] J. Verschraegen, M. Burgelman1, J. Penndorf, Thin Solid Films, 480–481, pp. 307–311, 2005.
[15] J. Van Gheluwe, J. Versluys, D. Poelman, J. Verschraegen, M. Burgelman, P. Clauws, Thin Solid Films, 511–512, pp. 304–308, 2006.
[16] M. Ben Rabeh, N. Khedmi, M. A Fodha , M. Kanzari, Energy Procedia 44, pp. 52–60, 2014 .
[17] M. Zribi, M. Kanzari, Thin Solid Films, 519, pp. 3865-3869, 2011.
[18] D. Abdelkader, N. Khemiri, M. Kanzari, Materials Science in Semiconductor Processing 16, pp. 1997–2004, 2013.
[19] M. Ben Rabeh, M. Kanzari, B. Rezig, Thin Solid Films, 515, pp. 5943–5948, 2007.
[20] J.M. Peza-Tapia, V.M. Sanchez-Resendiz, M.L. Albor-Aguilera, J.J. Cayente-Romero, L.R. De Leon-Gutierrez, M. Ortega-L pez, Thin Solid Films 490, pp. 142 – 145, 2005.
[21] T. Wen-Jen, T. Chia-Hung, C. Chih-Hui, T. Jyh-Ming, W. Rui-Ren, Thin Solid Films, 519, pp. 1712–1716, 2010.
[22] HP Klug, LE Alexander, X-ray Diffraction Procedures for Polycrystalline and Amorphous Materials. Wiley-Interscience. New York; pp. 594-597, 1974.
[23] O.S. Heavens, Optical Properties of Thin Solid Films; Butterworths: London, 1950.
[24] J. Tauc, Optical Properties of Solids, North Holand, Amsterdam, 1970.
[25] E.A. Davis, N.F. Mott, Philosophical Magazine, 22, pp. 903, 1970.
[26] W. Schottky, E. Spenke, Wiss. Veroff. Siemens-Werken, 18, pp. 225, 1939.
[27] S. Keraï, K. Ghaffour, N. E. Chabane-Sari, CISTEMA,2003.